

\bar{H}^+ Sympathetic Cooling Simulations with a Variable Time Step

Nicolas Sillitoe¹, Jean-Philippe Karr^{1,2}, Johannes Heinrich¹, Thomas Louvradoux¹, Albane Douillet^{1,2}, Laurent Hilico^{1,2}

¹ *Laboratoire Kastler Brossel, UPMC-Sorbonne Universités, CNRS, ENS-PSL Research University, Collège de France*

² *Dpt de Physique, Université d'Evry Val d'Essonne, 91025 EVRY France*

E-mail: laurent.hilico@lkb.upmc.fr

(Received May 19, 2016)

In this paper we present a new variable time step criterion for the velocity-Verlet algorithm allowing correct simulations of the dynamics of charged particles exchanging energy via coulomb collisions while minimising simulation time by varying the time step over orders of magnitude. We explain the need for such a criterion and we give one along with numerical results proving its validity. We numerically show that 1000 K \bar{H}^+ can be captured and sympathetically cooled by a crystal of Be^+ in less than 10 ms, an important result for the GBAR project.

KEYWORDS: Sympathetic Cooling

1. Introduction

A Paul Trap allows very long trapping times for ions, which in combination with cooling leads to applications in fields such as high resolution spectroscopy [5, 6], quantum computation and quantum simulations [7] and cold chemistry [4, 8]. Some ions such as $^9Be^+$ can be conveniently laser cooled [1, 2], most, however, cannot. One way to overcome this is sympathetic cooling whereby instead of trapping only the specie of interest another specie, which can be laser cooled, is also trapped. The specie which cannot be laser cooled will thermalise via coulomb interaction with the other specie, forming a cold two component coulomb crystal with a temperature bounded by the Doppler cooling limit, e.g. 0.47 mK or 60 neV in the case of Be^+ . Sometimes the ions cannot be created in situ and therefore have to be externally loaded at relatively high energies of 0.1-10 eV. Such is the case of highly charged ions [9] and antimatter ions [10] that are (or will be) created in heavy machinery and are of interest for fundamental physics experiments. One such experiment is the GBAR experiment which aims to cool \bar{H}^+ ions made of an antiproton and two positrons at CERN and study their free-fall to measure the gravity \bar{g} on antimatter [3, 11, 12].

One crucial step of the GBAR project is the capture and sympathetic cooling of \bar{H}^+ ions, so it is important to accurately evaluate the sympathetic cooling time by a laser cooled Be^+ ion crystal. Sympathetic cooling of externally loaded ions has been recently achieved for Ar^{13+} [9, 16] but the dynamics of the process have been little studied so far [15] especially for the case of very different mass-to-charge ratios as is the case in GBAR (9:1) [17]. Our goal is to numerically study this Doppler-cooling step. In Sec. 2, we briefly introduce the numerical model used for the simulations. In Sec. 3, we discuss the choice of the simulation time step and propose a new scheme to well describe Coulomb interactions that lead to sympathetic cooling. In Sec. 4, we discuss our first numerical results showing that \bar{H}^+ can be cooled by a laser cooled Be^+ ion crystal.

2. Ion crystal dynamics model

For the GBAR experiment, the idea [11] is to sympathetically cool a high velocity $\bar{\text{H}}^+$ ion using a laser cooled trapped Be^+ ion crystal. In a linear RF Paul trap, a laser cooled ion crystal in the Coulomb crystal regime has an ellipsoidal shape [13] as shown in Fig 1. The inter-ion distance is a few tens of microns and the crystal has at most few mm dimensions, depending on the ion number N . We therefore have a low density mesoscopic system which would be poorly described by mean-field methods so we cannot use $N\log N$ approximate methods [14] for the Coulomb interaction and we have to exactly compute it using the N^2 all-pairs approach. In order to well describe the crystal

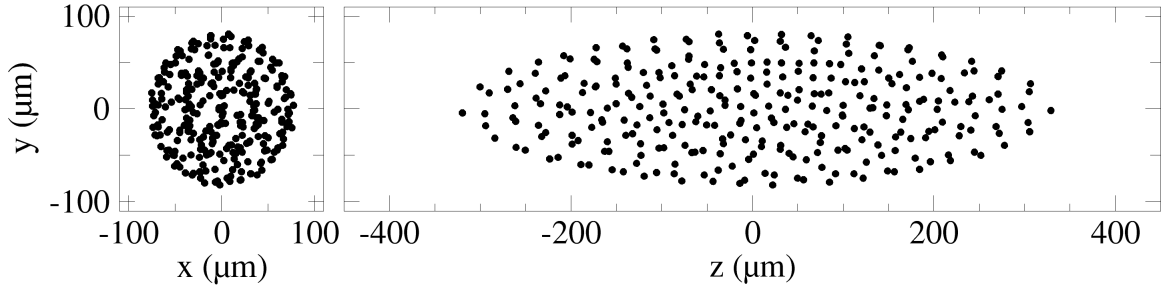


Figure 1. Projection of a simulated 300 Be^+ ion crystal in the xy (left) and zy (right) planes.

shape and dynamical properties, we solve Newton's equations including the time dependant confinement electric fields of the linear trap, the exact Coulomb force between all ion pairs and the laser interaction [?, ?, 21–24].

The confinement field derives from the potential [17]

$$V(x, y, z, t) = (U_0 + V_{\text{RF}} \cos(\Omega t)) \frac{x^2 - y^2}{2r_0^2} + m_i \omega_{i,z}^2 (z^2 - (x^2 + y^2)/2), \quad (1)$$

including the radial confinement in the x and y directions with $U_0=0.1$ V, $V_{\text{RF}}=200$ V, $r_0=3.5$ mm, $\Omega=2\pi \times 13$ MHz. The longitudinal confinement in the z direction is described in terms of axial oscillation frequency $\omega_z=2\pi \times 300$ kHz for $\bar{\text{H}}^+$ and 3 times less for $^9\text{Be}^+$.

We describe the interaction with the cooling laser as a stochastic process of absorption (depending on the ion's velocity through Doppler effect) spontaneous and stimulated emission, adding the corresponding velocity kicks to the laser cooled ions [18, 19]. The laser cooling beam is aligned with the trap axis. The waist of 1 mm is located at the trap center. The laser detuning is $-\Gamma$ where $\Gamma=19$ MHz is the width of the Be^+ cooling transition and laser intensity is 1.5 saturation intensity.

The ion crystal evolution is computed using the velocity-Verlet algorithm [20] given by

$$\begin{cases} x_i \\ a_i \\ v_i \end{cases} \rightarrow \begin{cases} x_{i+1} = x_i + v_i \delta t + \frac{a_i \delta t^2}{2} \\ a_{i+1} = F(x_{i+1}) \\ v_{i+1} = v_i + \frac{a_i + a_{i+1}}{2} \delta t \end{cases} \quad (2)$$

where $x_i = x(t_i)$, $v_i = v(t_i + \delta t/2)$, $a_i = a(t_i)$ and $F(x_i, t_i)$ is the force at time t_i . δt is the integration time step.

3. Choice of the integration time step

To accurately describe the Radio Frequency trapping potential (RF) of the Paul trap the integration time step δt needs to verify

$$\delta t \ll 2\pi/\Omega \quad (3)$$

As we will show, the proper description of coulomb interactions between ions can lead to time steps orders of magnitude smaller than what Eq. 3 prescribes. Equation 3 therefore gives an upper bound on the time step that can be used. We set it to 0.2 ns in our simulations performed with $\Omega=2\pi \times 13$ MHz. The description of laser cooling in terms of random absorption and emission events imposes time step much larger than the optical period, otherwise one would have to describe the laser interaction in terms of Bloch equation as discussed in [19]. For Be^+ cooling at 313 nm, the optical period is 1 fs, so the time step can be adapted over several orders of magnitude.

3.1 Coulomb interaction simulations with a fixed time step

In Figure 2 we consider a Coulomb collision between two particles and illustrate that for too long of a time step, a coulomb collision between two ions may be so poorly described that the two ions go through each other instead of repelling each other. To understand the time step requirements

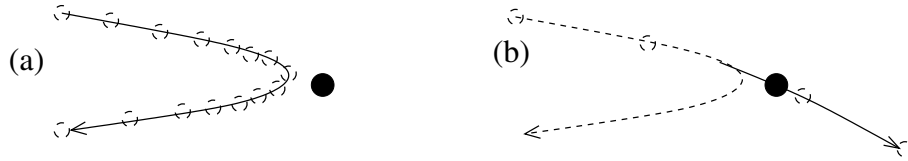


Figure 2. Coulomb collision between two ions in the frame of the target ion. (a) The time step is short enough and the collision is well described. (b) The time step is too long and the ions go through each other instead of repelling each other.

of simulating the coulomb interaction we simulated head-on 1D Coulomb collisions of two ions of equal mass and initially separated by 1 mm using a constant time step velocity-Verlet algorithm in the absence of the trapping field and the laser interaction. We send one ion at a given energy onto the other ion at rest. This problem has an analytical solution which predicts that the projectile ion transfers all its kinetic energy to the second ion.

In Fig. 3 we show the energy of the projectile ion after the collision versus time step for different projectile energies. At a given projectile energy we can see that for too long of a time step the ions don't exchange much energy. However, there is a threshold time step below which we can reproduce the expected result of the projectile ion losing all its energy. Notice the intermediate regime where the time step is close to being small enough, the outgoing energy of the projectile ion can fluctuate quite wildly as the ions can come closer than their minimum approach distance, numerically adding potential energy to the system.

We can interpret the threshold time step by saying that in a time step the ions should move much less than their minimum approach distance. At the beginning of the collision most of the mechanical energy is in the kinetic energy E_{in} of the projectile ion going at speed v_{in} in the lab reference frame. The minimum approach distance d_{min} is therefore given by

$$d_{min} = \frac{q_1 q_2}{2\pi\epsilon_0 \mu v_{in}^2} = \frac{q_1 q_2}{\pi\epsilon_0 m v_{in}^2} \quad (4)$$

with q_1, q_2 the charges of the two ions and $\mu = m/2$ the reduced mass. The displacement should obey

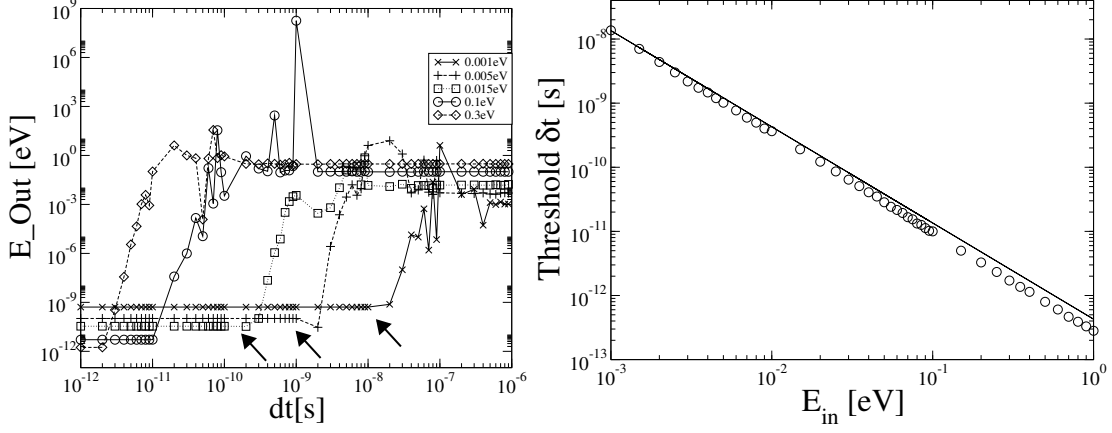


Figure 3. Left: Outgoing energy of a projectile ion after colliding with a stationary ion of equal mass for different projectile ion energies versus the constant time step used to simulate the collision. Arrows indicate the threshold time step below which the collision is well described. Right: The open circles show the threshold time step versus projectile initial kinetic energy, solid line is a fit to $\delta t = cE_{in}^{-\frac{3}{2}}$. Both curves consider collisions of two particles of mass 9 starting 1mm away.

$\delta r \approx v \delta t \ll d_{min}$ leading to

$$\delta t \ll \frac{q_1 q_2}{\pi \epsilon_0 m v_{in}^3} = \frac{q_1 q_2 \sqrt{m}}{\sqrt{8} \pi \epsilon_0} E_{in}^{-\frac{3}{2}} \quad (5)$$

where we have obtained the right hand side of the equation by upper bounding the relative speed of the two ions v by v_{in} . We have fitted the threshold energies found by such simulations to $\delta t = cE_{in}^{-\frac{3}{2}}$ and have found excellent agreement, finding that c should be approximately 4 times smaller than the right hand side of Eq. 5 for correct simulations. Figure 3 shows that the threshold time step is as small as 1 ps for only 0.3 eV of initial kinetic energy. This makes sympathetic cooling simulations of high temperature particles with a constant time step extremely demanding.

3.2 Variable time step criterion

Realistic dynamics of an ion crystal may involve fast ions and require very short time steps, e.g. if collisions with neutrals or exothermic reactions take place or as in the present case, if a fast ion is injected in a cold ion crystal to be sympathetically cooled. In this section, we show that a variable time step scheme allows us to have much longer time steps on average while accurately describing Coulomb interactions.

From the ideas of Sec. 3.1, we say that at every time step, for every ion pair, the relative change in distance δd_{ij} should obey

$$\delta d_{ij} \ll d_{ij} \quad (6)$$

with d_{ij} the distance between the two ions. We can reformulate the inequality in Eq. 6 as

$$\delta d_{ij} = \alpha d_{ij} \quad (7)$$

with α a constant to be chosen such that $\alpha \ll 1$. For velocity-Verlet integration position updates are given by

$$\delta \mathbf{r}_i = \mathbf{v}_i \delta t + \frac{1}{2} \mathbf{a}_i \delta t^2 \quad (8)$$

therefore the displacement d_{ij} between two ions is upper bounded by

$$\delta d_{ij} \leq \|v_{ij}\| \delta t + \frac{1}{2} \|a_{ij}\| \delta t^2 \quad (9)$$

with v_{ij} and a_{ij} the relative velocity and acceleration. Inserting Eq. 9 in Eq. 7 and solving the second degree equation for δt one finds the following time step

$$\delta t_{ij} = \frac{-\|v_{ij}\| + \sqrt{\|v_{ij}\|^2 + 2\|a_{ij}\| \alpha d_{ij}}}{\|a_{ij}\|}. \quad (10)$$

Equation 10 is specific to the case of a Velocity Verlet integration. Indeed, have found that evaluating δd_{ij} by $\|v_{ij}\| \delta t$ wasn't sufficient to describe a coulomb interaction because as the ions approach their minimal approach distance and as the velocity $\|v_{ij}\|$ vanishes the second term $\frac{1}{2} \|a_{ij}\| \delta t^2$ in Eq. 9 can no longer be neglected.

The variable time step scheme is therefore to apply Eq. 10 to every ion pair and to update δt at every time step using

$$\delta t = \min_{i,j} \delta t_{i,j}. \quad (11)$$

The all pairs computation of this variable time step scheme can be done "on the fly" while evaluating the Coulomb force but it adds a lot of computation to the already expensive $O(N^2)$ Coulomb evaluations because it involves three more square roots. Also, it requires more data transfers than the coulomb force evaluations because it involves not only the particles' positions, but also their speeds and accelerations. This variable time step scheme slows down the code by a factor of ~ 3 .

To verify this time step scheme, we simulated head-on 1D collisions of two ions with no trapping force nor laser cooling. We varied the parameter α from 1 down to $\frac{1}{5000}$. In Fig. 4 every point shows the maximum value of the ratio of the outgoing energy to the incoming energy of the projectile ion E_{out}/E_{in} over 20000 simulations with collision energies in a geometric progression from 0.1 meV to 1 eV. For $\alpha \gtrsim 1$ the time step is too long and the ratio is far from the analytically expected result of zero but as α decreases, the ratio rapidly converges to zero. In Sec. 4, we use $\alpha = 1/2000$, which insures an accurate description of the Coulomb collisions.

As a side note, one may elect to simulate at a constant time step such that Eq. 7 is valid for all ion pairs at all time steps. This may be achieved if the energy of any ion has an upper bound, known in advance, during the duration of a simulation. In the case of ion crystals in a linear Paul trap this is somewhat dangerous as the time varying RF field can increase the energy of the ions via so-called RF heating but a conservative upper-bound should still be possible as long as the heating doesn't diverge. One could also upper bound relative velocities and accelerations to twice the maximum velocity and twice the maximum acceleration respectively, and lower bound the distance between two ions by the lowest distance found during the calculation of the coulomb interaction. That way one could bring down the additional computational cost of the time step calculation to $O(N)$ at the cost of smaller time steps.

4. \bar{H}^+ sympathetic cooling

In this section, we study the capture and sympathetic cooling of a \bar{H}^+ ion by a cloud of 300 laser cooled Be^+ ions. We have performed 10 simulations by varying the random number series used for ion position initialisation and laser interaction. They all give very similar results. One of them is detailed in Fig. 5. The simulation first thermalises the 300 Be^+ ions using laser cooling (not shown in Fig. 5) leading to the ion crystal shown in Fig. 1. At $t = 3 \times 10^{-4}$ s, the projectile \bar{H}^+ ion is added at rest close to the trap axis at $x_0 = y_0 = 0$ with a standard deviation $\Delta x_0 = \Delta y_0 = 5 \mu m$ and $z_0 = 3 mm$

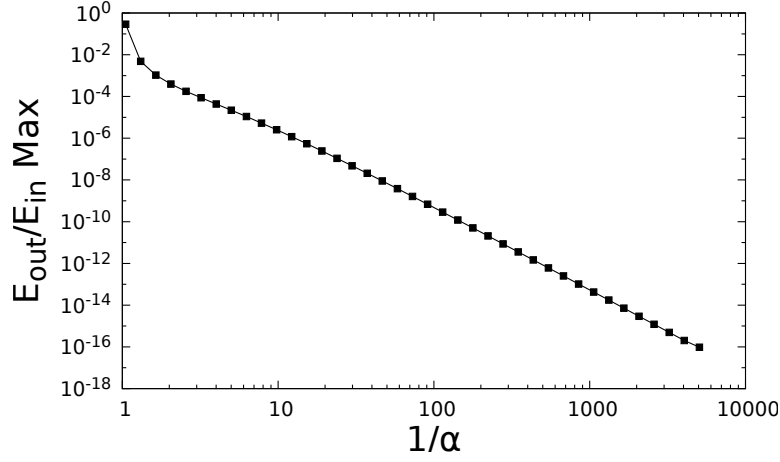


Figure 4. Maximum of the ratio of the outgoing energy to the incoming energy E_{out}/E_{in} of the projectile ion after a head-on collision obtained in a 1D model. The maximum is computed over 20000 collisions ranging from 0.1 meV to 1 eV. The ions start 10 cm away.

with a standard deviation $\Delta z_0 = 0.1$ mm corresponding to an initial potential energy of 167 meV. Figure 5 shows that the projectile ion oscillates back and forth through the Be^+ ion crystal for several ms before being captured and cooled by the Be^+ ion crystal. When the oscillation amplitude is large, the projectile ion spends most of the time out of the Be^+ ion crystal where its mechanical energy is preserved. Figure 5(d) shows that $v_z(t)$ oscillates with a flat top behaviour corresponding to the Be^+ crystal crossing. This is due to the fact that inside the ion crystal, the total electric field (trapping + Coulomb) is essentially zero such that the projectile ion does not feel any force. Figure 5(e) is a zoom on the flat top region. It shows that v_z fluctuates due to collisions with the trapped Be^+ ions. The net effect of the Be^+ crystal crossing is a slight decrease of the projectile axial velocity that results in projectile capture after many crossings. Indeed, once the axial projectile amplitude has decreased down to the dimensions of the Be^+ ion crystal, the interaction with the crystal becomes permanent and the projectile energy is quickly damped.

While the integration algorithm updates the time step at each time step, Figure 5(f) shows a coarse grain view of the time step evolution with time. The solid and dashed lines correspond to the minimum and average time step over 10 ns time intervals. The minimum time step fluctuates due to Coulomb interactions within the Be^+ ion crystal. One can see that when the projectile crosses the crystal, the time step is significantly reduced because the fast ion can come close to the Be^+ ions.

Figure 5(a) shows the trajectories of the projectile ion in the radial plane. Figure 6(a) shows the x , y and z contributions to the mean macro-motion kinetic energy (expressed in Kelvin) of the Be^+ ions and Fig. 6(b) those of the projectile ion. One can see that the kinetic energy lost by the projectile ion when crossing the ion crystal is partly transferred into radial kinetic energy and also directly to the Be^+ ion cloud explaining the spikes in the Be^+ temperature. This energy is damped by the laser cooling process with a few ms scale leading to cooling of all projectile degrees of freedom and a stable behaviour. The projectile ion temperature slowly decays from more than one thousand K down to the mK regime in less than 10 ms. One can notice that the Be^+ mean temperature is about 1 mK slightly above the Doppler limit because most of the Be^+ ions are off axis and undergo to micromotion while the $\bar{\text{H}}^+$ temperature is very close to the Doppler limit.

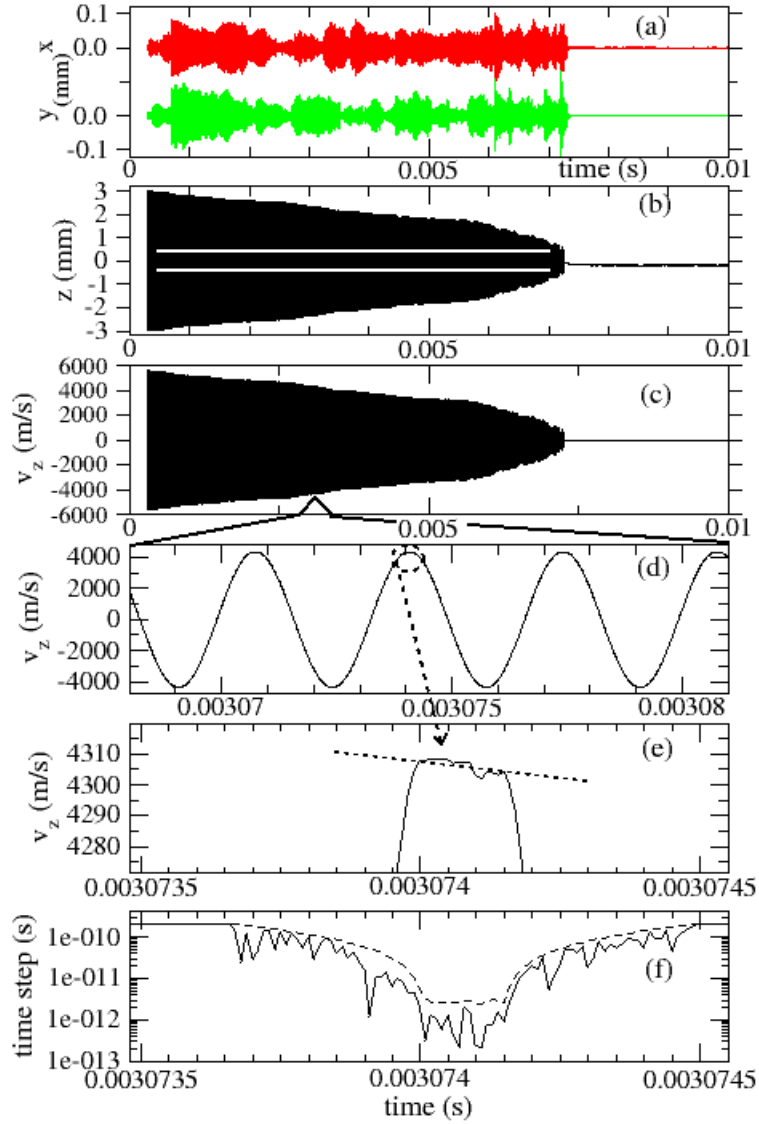


Figure 5. Trajectory of an $\bar{\text{H}}^+$ ion initially at rest at a distance $z_0 = 3$ mm from the center of the trap containing the Be^+ ion crystal shown in Fig.1. (a) $x(t)$ and $y(t)$ radial coordinates. (b) Axial position $z(t)$. The white lines indicates the longitudinal Be^+ ion crystal size. (c) Axial velocity $v_z(t)$. (d) Detail of $v_z(t)$ showing oscillations as the $\bar{\text{H}}^+$ ion goes back and forth through the ion crystal. (e) Detail of $v_z(t)$ showing that the $\bar{\text{H}}^+$ ion is slowed down while crossing the Be^+ ion crystal. (f) Minimum (solid line) and average (dashed line) time step per 10^{-8} s interval.

5. Conclusion

We have shown that simulating ionic interactions incurs a requirement on the time step to properly describe the coulomb interaction for which we have proposed and tested a variable time step scheme.

Using this scheme, we have performed accurate numerical simulations of sympathetic cooling of an $\bar{\text{H}}^+$ ion by laser cooled Be^+ ions, showing that sympathetic cooling can be performed in less than 10 ms for a initial kinetic energy of 167 meV (more than 1000 K). This result is very important to assess the feasibility of the Doppler sympathetic cooling step in the GBAR project. We will pursue

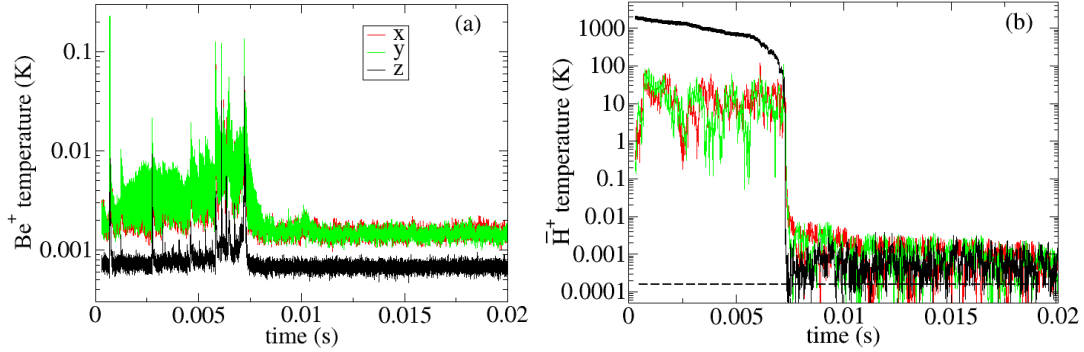


Figure 6. (a) Time evolution of the mean Be⁺ cloud macro-motion kinetic energy along the x , y and z directions obtained by averaging the velocities over one RF period. (b) Same quantities for the H⁺ projectile ion, but obtained by averaging over 10 RF periods to increase the lisibility of the curve. The horizontal dashed line indicates the Be⁺ Doppler limit per degree of freedom, i.e. 0.16 mK.

these simulations to determine the dependence of the cooling time to the initial energy of the H⁺ injected into the laser cooled crystal of Be⁺, and on the size of the Be⁺ ion cloud.

6. Acknowledgements

This work was supported by the ANR-13-IS04-0002-01 BESCOOL grant and the COMIQ ITN. J.-Ph. Karr acknowledges Institut Universitaire de France.

References

- [1] D.J. Wineland et al., PRL **40** (1978) 1639. *Radiation-Pressure Cooling of Bound Resonant Absorbers*.
- [2] W. Nauhauser et al., PRL **41** (1978) 233. *Optical-Sideband Cooling of Visible Atom Cloud Confined in Parabolic Well*.
- [3] P. Indelicato et al. (GBAR collaboration) Hyperfine Interactions **228** (2014) 141. *The GBAR project, or how does antimatter fall?*
- [4] S. Willitsch, Int. Rev. Phys. Chem **31** (2012) 175-199.
- [5] J. C. J. Koelemeij, B. Roth, A. Wicht, I. Ernsting, S. Schiller, Phys. Rev. Lett **98** (2007) 173002.
- [6] J. Biesheuvel, J.-Ph. Karr, L. Hilico, K. S. E. Eikema, W. Ubachs, J. C. J. Koelemeij, Nature Communications **8** (2016) 10385.
- [7] R. Blatt, C. Roos, Nature Physics **8** (2012) 277.
- [8] P. Eberle, A.D. Dörfler, C. von Planta, R. Krishnamurthy, D. Haas, D. Zhang, S.Y. T. van de Meerakker, S. Willitsch, J. Phys. Conf. Ser. **635** (2015) 012012.
- [9] L. Schmöger, O. O. Versolato, M. Schwarz, M. Kohnen, A. Windberger, B. Piest, S. Feuchtenbeiner, J. Pedregosa-Gutierrez, T. Leopold, P. Micke, A. K. Hansen, T. M. Baumann, M. Drewsen, J. Ullrich, P. O. Schmidt, J. R. Crespo Lopez-Urrutia, Science **347** (2015) 1233. *Coulomb crystallization of highly charged ions*.
- [10] P. Pérez and GBAR collab., Hyp. Int. **233** (2015) 21.
- [11] J. Walz, Th. Hänisch, General Relativity and Gravitation **36** (2004) 561.
- [12] P. Prez, Y. Sacquin, Classical and Quantum Gravity **29** (2012) 18.
- [13] L. Turner, Phys. Fluids **30** (1987) 3196.
- [14] B. Chapman & al., Parallel Computing : from Multicores and GPU's to Petascale, IOS Press (2010). DOI:10.3233/978-1-60750-530-3-323
- [15] M. Bussmann, U. Schramm, D. Habs, V.S. Kolhinen, J. Szerypo, Int. J. Mass Spectrometry **251** (2006) 179.

- [16] L. Schmöger, M. Schwarz, Th. M. Baumann, O. Versolato, B. Piest, T. Pfeifer, J. Ullrich, P. O. Schmidt, and J. R. Crespo Lopez-Urrutia Rev. Scient. Instr. **86** (2015) 103111. *Deceleration, precooling, and multi-pass stopping of highly charged ions in Be^+ Coulomb crystals.*
- [17] L. Hilico, J.-Ph. Karr, Albane Douillet, P. Indelicato, S. Wolf, F. Schmidt Kaler, , Int. J. Mod. Phys. Conference Series **30** (2014) 1460269. *Preparing single ultra-cold antihydrogen atoms for the free-fall in GBAR.*
- [18] Physics with charged trapped particles, Ed. M. Knoop, N. Madsen, R. Thompson, World Scientific (2016), Chap. 8 by N. Sillitoe and L. Hilico, Numerical simulations of ion cloud dynamics.
- [19] I. Rouse, S. Willitsch, Phys. Rev. A **92** (2015) 053420.
- [20] Loup Verlet, Phys. Rev. **159** (1967) 98. *Computer "Experiments" on Classical Fluids. I. Thermodynamical Properties of Lennard-Jones Molecules.*
- [21] C. B. Zhang, D. Offenberger, B. Roth, M. A. Wilson, S. Schiller, PRA **76**, (2007) 012719. *Molecular-dynamics simulations of cold single-species and multispecies ion ensembles in a linear Paul trap.*
- [22] S. Schiller, C. Lämmerzahl, PRA **68**, (2003) 053406. *Molecular dynamics simulation of sympathetic crystallization of molecular ions.*
- [23] K. Okada, M. Wada, T. Takayanagi, S. Ohtani, H. A. Schuessler, PRA **68**, (2003) 053406. *Characterization of ion Coulomb crystals in a linear Paul trap.*
- [24] M. Marciante, C. Champenois, A. Calisti, J. Pedregosa-Gutierrez and M. Knoop, Phys. Rev. A. **82** (2010) 033406. *Ion dynamics in a linear radio-frequency trap with a single cooling laser.*